THE EUROPEAN SOCIETY OF MEDICINE
Medical Research Archives, Volume 14 Issue 3

RESEARCH ARTICLE

Thalamocortical projections to the premotor cortex following unilateral lesion of the primary motor cortex in macaque monkeys.

Adjia Hamadjida [1,2,3], **Eric M. Rouiller** [1]

[1] Department of Neurosciences and Movement Sciences, Section of Medicine, Faculty of Sciences and Medicine, University of Fribourg, Chemin du Musée 5, CH-1700 Fribourg, Switzerland.
[2] Department of Neurosciences, Section of Medicine, Faculty of Sciences, University of Saint Boniface, Winnipeg, Canada.
[3] Department of Life Science, Higher Teacher Training College, University of Bertoua, Bertoua, Cameroon.

Dr. Adjia Hamadjida ORCID: 0000-0001-9869-6752
Prof. E.M. Rouiller ORCID: 0000-0003-1355-6019

OPEN ACCESS

PUBLISHED
31 March 2026

CITATION
Hamadjida, A., and Rouiller, EM., 2026. Thalamocortical projections to the premotor cortex following unilateral lesion of the primary motor cortex in macaque monkeys. Medical Research Archives, [online] 14(3).

ISSN
2375-1924

ABSTRACT

Voluntary movements, such manual dexterity with independent use of fingers, strongly depend on the corticomotoneuronal projection system in primates. Furthermore, the cortico-basal ganglia-thalamo-cortical and cortico-cerebello-thalamo-cortical loops contribute to shape motor commands for manual dexterity. The thalamocortical projections to multiple motor cortical areas represent a crucial terminal projection step underlying these two subcortical influences. The present study aimed at investigating whether the thalamocortical projection terminating in the premotor cortex is affected following a lesion restricted to the homolateral primary motor cortex in adult macaque monkeys. The thalamocortical projections to the premotor cortex were compared between intact monkeys (n=3) and monkeys subjected to a unilateral lesion of the homolateral primary motor cortex hand area (n=7), using the biotinylated dextran amine retrograde tract-tracing method. The group of 7 lesioned monkeys was subdivided into a subgroup of 4 untreated subjects, while a subgroup of 3 subjects was treated with an anti-Nogo-A antibody. The biotinylated dextran amine retrogradely labelled thalamocortical neurons projecting to the premotor cortex were charted and quantified across different thalamic nuclei. The absolute total numbers of thalamocortical stained neurons were considered for further analysis and inter-subgroups' comparison. As compared to intact monkeys, the thalamocortical projections' density in lesioned untreated monkeys was strongly reduced (about 6x less). In the anti-Nogo-A antibody treated subgroup (also lesioned), the density of thalamocortical projection was less reduced (about 3x), as compared to intact monkeys. To minimize interindividual variability related to the tracer injection sites' properties, the numbers of thalamocortical stained neurons were normalized in each monkey based on the numbers of biotinylated dextran amine labelled corticospinal axons. The normalization yielded comparable results as the absolute thalamocortical numbers, with however a more pronounced, actually complete separation between the 3 respective ranges of data points corresponding to the 3 monkeys' subgroups. In conclusion, the lesion of the primary motor cortex induced a sharp downregulation of thalamocortical projections to the homolesional premotor cortex, which was moderately minimized by the anti-Nogo-A antibody treatment.

Keywords: thalamocortical projection, thalamus, cortical lesion, anti-Nogo-A antibody, neuroplasticity, tract-tracing, motor control, non-human primates

Abbreviations

AD	anterior dorsal nucleus
AV	anterior ventral nucleus
BDA	biotinylated dextran amine
CL	central lateral nucleus
CeM	centromedial nucleus
CM	centromedian nucleus
CS	corticospinal
ICMS	intracortical microstimulation
LD	lateral dorsal nucleus
LP	lateral posterior nucleus
MD	mediodorsal nucleus
M1	primary motor cortical area
PC	paracentral nucleus
PU	pulvinar nucleus
PM	premotor cortex
PMd	dorsal premotor cortex
PMd-c	caudal part of PMd
PMd-r	rostral part of PMd
PMv	ventral premotor cortex
PMv-c	caudal part of PMv
PMv-r	rostral part of PMv
R	reticular nucleus
SMA	supplementary motor cortical area
TC	thalamocortical
VA	ventroanterior nucleus
VM	ventromedial nucleus
VL	ventrolateral nucleus
VP	ventroposterior nucleus
ZI	zona inserta

Introduction

In non-human primates, the multiplicity of motor cortical areas [1-9] and the corticomotoneuronal projection system [6,10-15] are key structures underlying the exquisite ability of primates to finely and independently control their fingers' movements, corresponding to manual dexterity [but see also 16,17]. Following a unilateral lesion of the hand area in the primary motor cortex (M1) in adult macaques, an acute phase of dramatic loss of manual dexterity of the contralesional hand follows, lasting a few weeks [e.g. 18-34]. A spontaneous, progressive functional recovery of manual dexterity then takes place, reaching a plateau of usually incomplete recovery. The intact ipsilesional premotor cortex (PM) plays an important role in the functional recovery from lesion of the primary motor cortex, in particular with a remodeling of its efferent and afferent projections [20,22,28,31,32,35-48].

Although the corticospinal projection is essential for manual dexterity, other motor pathways play a role in shaping the voluntary movements, in particular the cortico-basal ganglia-cortical and cortico-cerebellum-cortical loops [e.g.43,49-58]. The basal ganglia and the cerebellum receive efferent copies of the motor commands issued by the motor cortical areas, which are processed locally and then re-injected to the motor cortical areas of origin via the thalamus. The final step of these two loops thus includes a thalamocortical (TC) projection, in the form of pallido-thalamocortical and cerebello-thalamocortical projection systems [50,59-71]. As outlined above, after lesion of the primary motor cortex, the adjacent premotor cortex is strongly reorganized with respect to its efferent (cortico-supraspinal, corticospinal) and afferent (corticocortical) projections. What about its motor afferent inputs from the thalamus, i.e. the thalamocortical projections to the premotor cortex? As compared to intact monkeys, and following a unilateral lesion of the primary motor cortex, is the thalamocortical projection to the ipsilesional premotor cortex modified? If yes, is it downregulated or upregulated, reflecting a functional adaptation, possibly related to the incomplete functional recovery taking place a few months after the lesion of the primary motor cortex? Finally, what is the impact of an anti-Nogo-A antibody treatment on this thalamocortical projection to the premotor cortex, considering that this therapy enhanced the functional recovery of manual dexterity from the primary motor cortex lesion [27,28,33]? To address these questions, using the retrograde Biotinylated Dextran Amine (BDA) tract-tracing method, the origin and strength of the thalamocortical projections to the premotor cortex were established in 3 subgroups of monkeys: (i) 3 intact monkeys; (ii) 4 untreated monkeys subjected to a lesion of the primary motor cortex; (iii) 3 monkeys treated with the anti-Nogo-A antibody and also subjected to a lesion of the primary motor cortex.

Material and Methods

The present retrograde tracing data are derived from experiments conducted on 10 adult monkeys (Macaca fascicularis; Table 1), with ages ranging between 4 and 10 years (median=5 years old) and weights between 2.6 and 10 kg (median=4 Kg). All monkeys (MKs) were included in one or the other of our previous tract-tracing and/or primary motor cortex lesional investigations [20,27,28,33,39,47,48,72-77]. Surgical procedures and animal care (including housing in the animal facility: see www.unifr.ch/spccr/about/housing) were conducted in accordance with the Guide for the Care and Use of Laboratory Animals (ISBN 0-309-05377-3; 1996) and were approved by local (canton of Fribourg: "*commission de l'expérimentation animale*" et "*vétérinaire cantonal*") and federal (Swiss: "*office vétérinaire fédéral*") veterinary authorities (official authorizations FR 24/95/1; FR 44/92/3; FR 157/01, FR 157/03, FR 166-03, FR-166-05, FR 157/04, FR 156/04, FR 156/06, FR 157e/06; FR 206/08, FR 185-08, FR 192/07, FR 192/07E, 19017, 22010, 2014-FR-42E, FR 17-09, FR 18-10). In the animal facility specifically designed for non-human primates, groups of 2-5 monkeys were housed in a 45 m^3 room for each group. In addition, for each room, monkeys had access to an additional outdoor space (12-15 m^3). The monkeys had permanently free access to water in the animal facility and furthermore they were not food restricted.

The surgical procedures for unilateral permanent lesioning of the hand area in the primary motor cortex with infusion of ibotenic acid (including intracortical micro-stimulation procedures) and for the injections of the tracer Biotinylated Dextran Amine (BDA) in the premotor cortex were described in great detail earlier and are therefore not repeated here [20,26-28,34,39,78-87]. Biotinylated Dextran Amine is typically an anterograde tracer, but it can also be used as retrograde tracer, as

previously reported [39,78,79,82]. The anti-Nogo-A antibody treatment [84-86,88,89] was administered in 3 of the primary motor cortex lesioned monkeys (Table 1) as previously reported [27,28]. At the end of the experiment, the monkeys were euthanized and the brain tissue was prepared for histology as described earlier [78]. Frontal sections (50 µm thick) of the brain were then cut in the frontal plane and collected in five series. Biotinylated Dextran Amine staining was revealed in one series of sections [78]. A second series of sections was Nissl stained with cresyl violet, whereas a third series of sections was processed to visualize the marker SMI-32, as previously described [83,90-92]. Two remaining series of sections were kept in reserve. The Nissl and SMI-32 consecutive stained histological sections were used to reconstruct the position and extent of the permanent lesion in the primary motor cortex as previously reported [27,34,39,93], as well as to establish the parcellation of the thalamus, according to available cytoarchitectonic criteria and nomenclature [94-99]. The position and extent of the Biotinylated Dextran Amine injection sites in the dorsal premotor cortex (PMd) and/or in the ventral premotor cortex (PMv) were derived from the reconstruction of Biotinylated Dextran Amine stained sections (Table 1; [see also 39,72,74]). The same series of Biotinylated Dextran Amine stained sections allowed to establish the distributions of retrogradely BDA-labelled thalamocortical neurons in the ipsilateral thalamus, plotted with the aid of Neurolucida ™ (MicroBrighField, Inc, Colchester, VT, USA). The plotting of the Biotinylated Dextran Amine labelled neurons was done at 1 mm intervals (1 every 4 sections in the BDA series along the rostro-caudal axis), by visualizing and charting every individual neuron on each analysed section, corresponding to a quantification method based on exhaustive plotting, instead of stereology [72,74].

Images of plotted sections were processed using Corel Draw 14.0 software and labelled neurons were then superimposed on photomicrographs obtained from the corresponding Nissl and/or SMI-32 stained sections series (Figures 1 and 2). Typical BDA labelled thalamocortical neurons are illustrated in Figure 1 (panel J), showing also the presence of two gray halos, in the middle and on the upper right (arrows): they correspond to zones of dense axonal terminals emitted by the reciprocal corticothalamic projection, anterogradely labelled with BDA.

In addition, the number of BDA labelled corticospinal (CS) axons was determined, as previously reported [72,74], and used for the normalization procedure (Table 1): for each monkey, the total absolute number of BDA labelled thalamocortical neurons was divided by the number of BDA labelled CS axons * 1000 (Table 1). The same normalization procedure was applied in previous tract-tracing studies from this laboratory [39,47,48,72-77].

Table 1	Intact			M1 lesion - untreated				M1 lesion - treated with anti-Nogo-A antibody		
Monkey ID	**Mk-CH**	**Mk-R13**	**Mk-R12**	**Mk-CE**	**Mk-GE**	**Mk-RO**	**Mk-BI**	**Mk-VA**	**Mk-MO**	**Mk-LA**
Species	fasc.	fasc.	fasc.	fasc.	fasc.	fasc.	fasc.	fasc.	fasc.	fasc.
Sex	male	female	female	male	female	male	male	male	male	female
M1 Lesion	No	No	No	Yes [a]	Yes [a]	Yes [a]	Yes [a]	Yes [a]	Yes [a]	Yes [c]
M1 Lesion volume (mm^3)	-	-	-	112.8	48.7	14	20.13	20	41.8	3.1
Treatment	None	None	None	None	None	None	None	Anti-Nogo-A	Anti-Nogo-A	Anti-Nogo-A
Age at lesion (rounded 0.5 year)	10	4.5	5	4.5	5	4	5	5.5	5.5	5
Weight at lesion (Kg)	6#	4#	4#	3.8	2.8	3.2	5	4.9	5.6	2.6
Volume of BDA injected (µL)	8	8.8	7.2	16	2.1	4.8	7.2	5	10.8	2
Nb. BDA injected sites in PM	10	11	9	16	5	6	11	5	12	5
PM areas injected with BDA	PMd/PMv[b]	PMd/PMv[b]	PMd [b]	PMd [a]	PMd/PMv[a]	PMd [a]	PMd/PMv [a]	PMd/PMv [a]	PMd/PMv[a]	PMd/PMv [c]
Nb. BDA labelled TC cells	**3950**	**4157**	**1842**	**735**	**716**	**242**	**792**	**1602**	**1927**	**618**
Nb. of BDA labelled CS axons	1201	1802	1473	1810	885	543	1328	1312	1975	763
Normalized Nb. BDA lab. TC cells &	**3289**	**2307**	**1251**	**406**	**809**	**446**	**596**	**1221**	**976**	**810**

& Normalization procedure: see methods. See also list of abbreviations.

[a] the position and extent of the M1 lesion and of the BDA injection site in those monkeys can be seen in Hamadjida et al., 2012 [39].

[b] the position and extent of the BDA injection site can be seen in Fregosi et al., 2017 [72].

[c] the position and extent of the M1 lesion and of the BDA injection site in Mk-LA can be seen in Figure 2J (see also Gindrat et al., 2025 [77]).

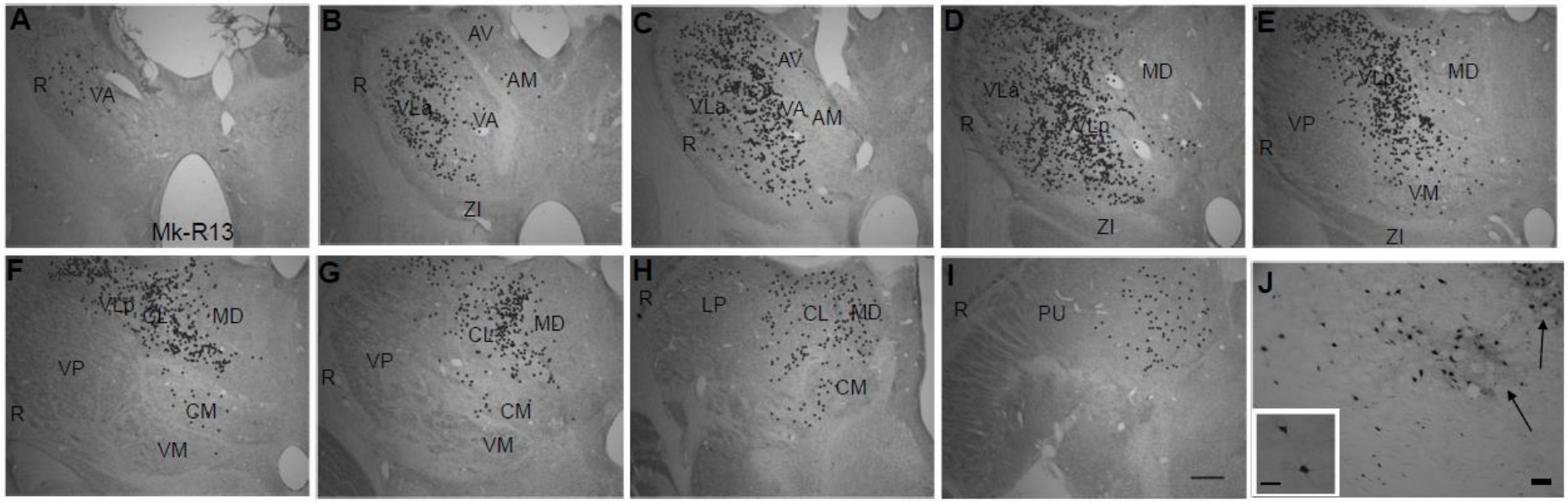

Figure 1

Panels A to I: Nissl-stained frontal sections of the thalamus, from rostral (A) to caudal (I), 1 mm interval (Mk-R13). Scale bar: 1 mm. The superimposed black dots display the BDA labelled thalamocortical neurons. See list of abbreviations and Table 2 for the nomenclature of thalamic nuclei.

Panel J: Photomicrograph of BDA retrogradely labelled thalamocortical neurons (dark spots; scale bar: 100 mm). The inset on the bottom left is an enlargement, showing 2 labelled neurons (scale bar=50 mm). See text for the description of halos pointed by the 2 arrows.

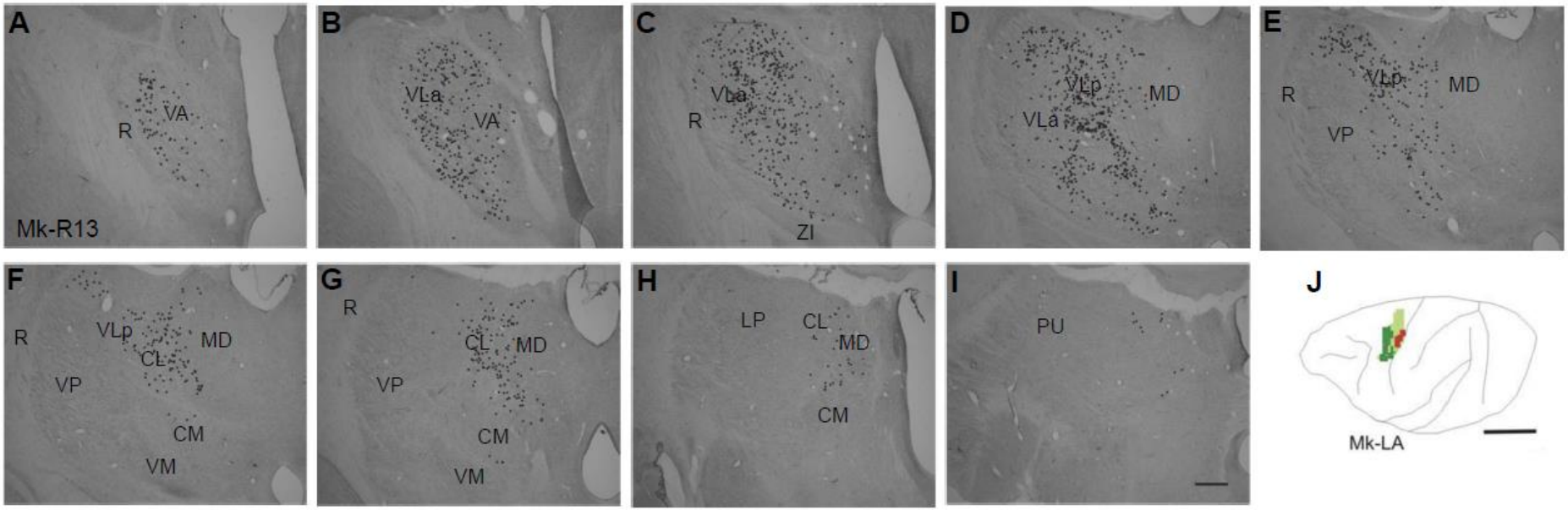

Figure 2

Panels A to I: Nissl-stained frontal sections of the thalamus, from rostral (A) to caudal (I), 1 mm interval (M1 lesioned Mk-MO). Scale bar: 1 mm. Same conventions as in Figure 1. Panel J: Lateral view of the left hemisphere of Mk-LA, with position and extent of the M1 lesion (red area) and of the BDA injection site in the premotor cortex (dark green spot for the core of the injection site and pale green spot for the halo, not published before). Scale bar: 10 mm.

Results

The BDA tract-tracing experiments were conducted on 10 adult macaques, as listed in Table 1. The latter (bottom lines) also indicates the precise articles from this laboratory in which the primary motor cortex lesion extent and position were displayed for each of the 7 individual monkeys subjected to such lesion. The volume of the primary motor cortex lesion for each monkey is reminded in Table 1. Three of the 7 monkeys subjected to the unilateral primary motor cortex lesion received an anti-Nogo-A antibody treatment, which enhanced the functional recovery of manual dexterity, as compared to untreated monkeys [27,28,33]. Table 1 also indicates the previously published articles in which the BDA injection sites were reconstructed and displayed for each of the 10 monkeys (including the 3 intact ones), except Mk-LA whose injection site is shown in Figure 2 (panel J). As a result of BDA injection in the premotor cortex (in PMd and PMv, or in PMd alone: see Table 1), retrogradely labelled neurons were observed and charted in the ipsilateral thalamus, corresponding to thalamocortical neurons (Figs. 1 and 2). The numbers of thalamocortical stained neurons were established in the different subdivisions of the thalamus, a distribution expressed in percentages (Table 2). As expected, the vast majority of BDA labelled thalamocortical neurons were located in the ventral group (range 69-92% across monkeys), mostly in the ventrolateral nucleus of the thalamus. The number of BDA labelled thalamocortical neurons was significant and fairly consistent across monkeys in the medial group (range 5-16%), while it was more variable inter-individually and, in most cases smaller in the other thalamic groups (anterior, lateral and intralaminar).

Further quantitative analysis was conducted on the total numbers of BDA labelled thalamocortical neurons in each monkey (Table 1). As shown in Figure 3 (left part of the graph), these absolute total numbers show a largely segregated distribution of these data points across the 3 subgroups of monkeys. As a result of the primary motor cortex lesion, the 4 untreated monkeys exhibited a dramatic decrease of the numbers of labelled thalamocortical neurons (range 242 to 792), in comparison to the 3 intact monkeys (range 1842 to 4157). In 3 other primary motor cortex lesioned monkeys, but subjected to an anti-Nogo-A antibody treatment, the strong decrease of the numbers of thalamocortical labelled neurons due to the lesion was somewhat attenuated by the treatment (range 618 to 1927).

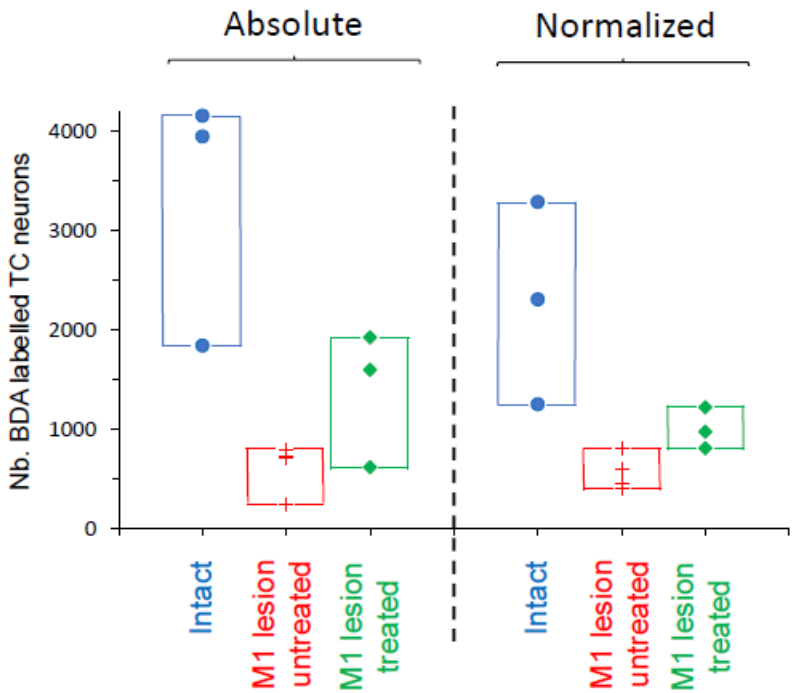

Figure 3

For each monkey, distribution of the numbers of BDA labelled thalamocortical neurons, given by their absolute numbers (left half of the graph) or by normalized numbers (right half of the graph), for the 3 subgroups of monkeys distinguished by different colors and distinct symbols. For each subgroup, the rectangle indicates the dispersion of the data points. The corresponding data points are listed in Table 1.

Table 2: Percentages of BDA thalamocortical labelled cells in the various thalamic groups and nuclei (intact and M1 lesion monkeys)

Thalamic groups / nuclei		Intact			M1 lesion / Untreated				M1 lesion / Anti-Nogo-A Treated		
		Mk-CH	**Mk-R13**	**Mk-R12**	**Mk-CE**	**Mk-GE**	**Mk-RO**	**Mk-BI**	**Mk-VA**	**Mk-MO**	**Mk-LA**
Anterior group	AM	1.11	0.1	0	0	0	0	0	0.37	0.67	0
	AV	1.42	0.31	0	0.14	0	0	0	0.12	1.45	0
	AD	0.23	0	0	0.68	0	0	0	0	0	0
	LD	0.58	0.72	0.05	0.14	0	0.83	0.25	0.44	0	0.16
	Sub-Total	**3.34**	**1.13**	**0.05**	**0.96**	**0**	**0.83**	**0.25**	**0.93**	**2.12**	**0.16**
Ventral group	VA	24.53	16.91	6.73	10.75	2.93	1.24	4.04	3.68	15.2	3.4
	VL	36.28	52.66	64.93	52.11	73.04	78.51	79.42	58.55	60.98	76.86
	VM	6.99	5.92	0.16	2.58	3.35	0	5.81	5.12	5.35	1.78
	VP	1.44	0.43	2.5	6.39	6.15	0	2.27	9.11	0	2.75
	Sub-Total	**69.24**	**75.92**	**74.32**	**71.83**	**85.47**	**79.75**	**91.54**	**76.46**	**81.53**	**84.79**
Lateral group	LP	3.27	2.98	9.5	2.04	0.28	0	0	3.37	2.7	0
	PU	4.78	1.23	2.33	10.48	0	0	0	2.75	0	0
	Sub-Total	**8.05**	**4.21**	**11.83**	**12.52**	**0.28**	**0**	**0**	**6.12**	**2.7**	**0**
Medial group	MD	13.19	14.05	10.8	5.71	10.2	16.11	8.21	4.68	10.43	11.65
	Sub-Total	**13.19**	**14.05**	**10.8**	**5.71**	**10.2**	**16.11**	**8.21**	**4.68**	**10.43**	**11.65**
Intralaminar group	PC	0.51	0.46	0	0	1.12	0	0	0.19	0.93	0
	CL	4.33	2.74	2.08	6.94	0.56	2.48	0	3.37	1.5	1.94
	CM	1.34	1.49	0.92	2.04	2.37	0.83	0	8.24	0.78	1.46
	Sub-Total	**6.18**	**4.69**	**3**	**8.98**	**4.05**	**3.31**	**0**	**11.8**	**3.21**	**3.4**
Total percentages		**100**	**100**	**100**	**100**	**100**	**100**	**100**	**100**	**100**	**100**
Total absolute mumbers		**3950**	**4157**	**1842**	**735**	**716**	**242**	**792**	**1602**	**1927**	**618**

AD: anterior dorsal nucleus; AM: anteromedial nucleus; AV: anterior ventral nucleus; CL: central lateral nucleus; CM: centromedian nucleus; LD: lateral dorsal nucleus; LP: lateral posterior nucleus; MD: mediodorsal nucleus; PC: paracentral nucleus; PU: pulvinar nucleus; VA: ventroanterior nucleus; VL: ventrolateral nucleus; VM: ventromedial nucleus; VP: ventroposterior nucleus

The absolute numbers of BDA-labelled thalamocortical neurons may be biased to some extent by the variability of several parameters related to the multiple injection sites, in particular the volume of BDA injected or the number of infusion sites (Table 1). To tentatively minorize the impact of this variability, a normalization procedure was introduced in earlier tract-tracing studies from this laboratory [47,48,72-76], based on the number of BDA-labelled corticospinal (CS) axons observed above the pyramidal decussation, and originating from layer V in the injected motor cortex. This normalization based on labelled corticospinal axons is relevant considering that the cortico-cerebellar-thalamo-cortical loop also takes its origin in layer V, via the efferent projections directed to pre-cerebellar nuclei (e.g. pontine nuclei). This may also apply to the cortico-striatal-pallido-thalamo-cortical loop, believed to originate from layer V as well.[100] However, more recent data showed that the origin of the corticostriatal projections from motor cortical areas is more complex, spread across layers III to VI [101]; Nevertheless, the layer V may still be representative, at least to some extent, of the output of the adjacent layers III and VI, directed to the striatum. The numbers of BDA-labelled corticospinal axons used for normalization are listed for each monkey in Table 1. For normalization, in each monkey the total number of thalamocortical labelled neurons was divided by the number of corticospinal axons, multiplied by 1000 (Table 1). The normalized numbers of BDA-labelled thalamocortical neurons were plotted in the right part of Figure 3. Although the effect of the normalization was not massive, it still enhanced the segregation between the 3 subgroups of monkeys, with an absence of overlap between the three corresponding ranges of data points. In addition, within each subgroup of monkeys, the normalization reduced the dispersion of the 3-4 data points (Fig. 3). To summarize the results of the present study, both the absolute and normalized data support the conclusion that, after a primary motor cortex lesion, the thalamocortical projection to the ipsilesional premotor cortex is strongly downregulated, as compared to intact monkeys, a reduction moderately minimized by the anti-Nogo-A antibody treatment. As shown in Figure 4, for the primary motor cortex lesioned monkeys (n=7), there was no obvious relationship between the absolute or normalized numbers of BDA-stained thalamocortical neurons after BDA injection in the ipsilesional premotor cortex and the primary motor cortex lesion volume. At least the possibly expected hypothesis that, the larger the primary motor cortex lesion volume the bigger its impact on thalamocortical cells' reduction, was not verified. Indeed, there was no progressive decrease of thalamocortical labelled neurons' numbers for increasing lesion volumes (Fig. 4). This observation is however based on a limited number of cases (n=7).

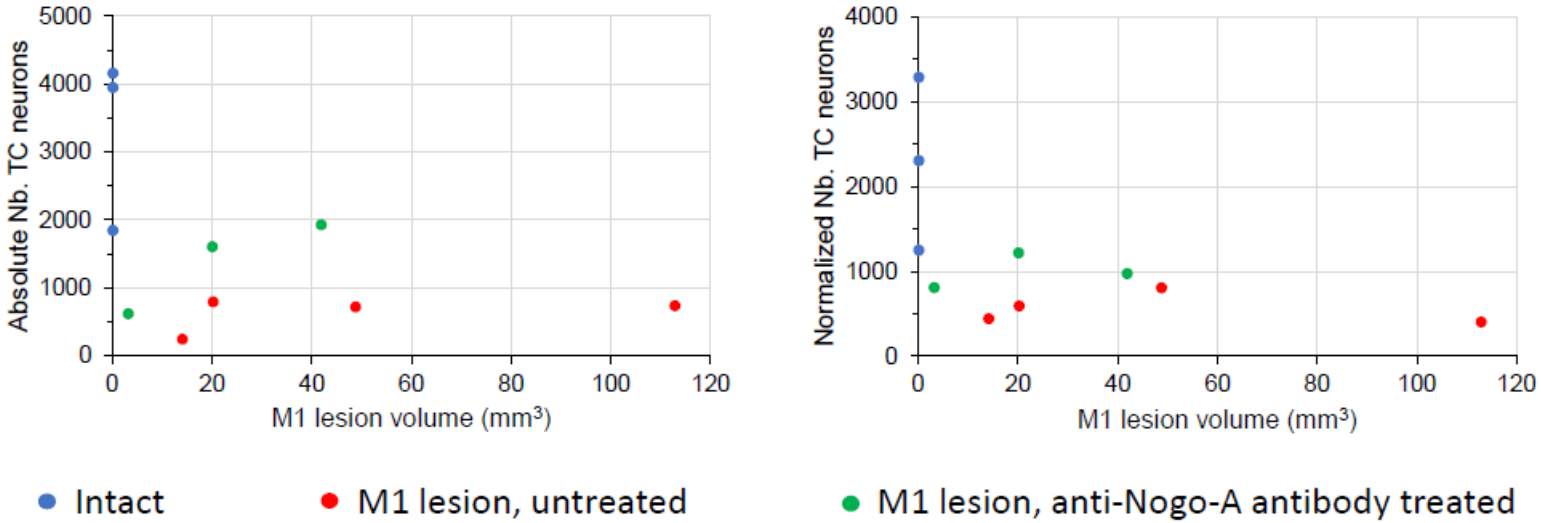

Figure 4

For the 7 monkeys subjected to the primary motor cortex lesion, the absolute (left graph) and the normalized (right graph) numbers of BDA-stained thalamocortical neurons (ordinate) were plotted as a function of the corresponding lesion volume (abscissa). The red symbols are for the 4 untreated monkeys while the green symbols are for the 3 anti-Nogo-A antibody treated monkeys. For comparison, the numbers of BDA-stained thalamocortical neurons observed in the 3 intact monkeys were plotted with blue symbols (lesion volume = 0). All corresponding individual data are listed in Table 1.

Discussion

The main result of the present study is the strong decrease of the thalamocortical projection terminating in the premotor cortex following homolateral lesion of the primary motor cortex in adult macaque monkeys. This original observation, as far as thalamocortical projection is concerned, adds a new element in the long list of changes affecting the efferent [43,47,48,74,75] and afferent [36,39] connections of the premotor cortex, following primary motor cortex lesion. The present decrease of thalamocortical projections to the premotor cortex in presence of primary motor cortex lesion is indeed accompanied by a strong decrease of the corticoreticular and corticorubral efferent projections from the premotor cortex, in nearly the same pool of monkeys [47,48,74]. Functionally, this effect would support the notion that after primary motor cortex lesion, the corresponding reticulospinal and rubrospinal projection systems may work more independently from the intact ipsilesional premotor cortex, an adaptation possibly involved in the incomplete spontaneous functional recovery of manual dexterity. In contrast, the rewiring of premotor cortex connections after primary motor cortex lesion involves an increase of sprouting and redirection of axons originating from the premotor cortex in the vicinity of the primary motor cortex lesion [36]. In addition, the premotor cortex was also reported to establish new connections (afferent and efferent) with the ipsilesional areas 1 and 2 of the primary somatosensory cortex [36]. Callosal afferent projections to the ipsilesional premotor cortex were on the other hand dowregulated [77]. On the functional point of view, the reduction of thalamocortical projections to the ipsilesional premotor cortex after primary motor cortex lesion reported here (Fig. 3) is consistent with a reduced influence on cortical motor control of the cortico-basal ganglia-thalamus-cortical and cortico-cerebellar-thalamus-cortical loops, considering that the final step of these loops, the thalamocortical projection, is believed to be excitatory. Overall, the parallel downregulations of the efferent supraspinal projections from the premotor cortex as well as of the influence of the basal ganglia and cerebellar loops suggest that post primary motor cortex lesion, the direct corticospinal projections from preserved ipsilesional or contralesional motor cortical areas (M1, PM, SMA) may be privileged in the form of an upregulation [102,103], in the context of spontaneous functional recovery of manual dexterity. With the present material (monkeys listed in Table 1), the next step in future investigations is to determine whether the corticospinal projection from the ipsilesional premotor cortex is indeed upregulated at terminal level in the cervical spinal cord in primary motor cortex lesion monkeys, in comparison to intact monkeys, with even a possible further enhancement resulting from anti-Nogo-A antibody treatment.

The anti-Nogo-A antibody treatment minimized the decrease of the thalamocortical projection to the premotor cortex after primary motor cortex lesion, contributing to a reversal to some extent toward the thalamocortical density projection prevailing in intact monkeys (Fig. 3). Behaviorally, the treatment enhanced the functional recovery of manual dexterity, by about 20-40% score improvement, as compared to untreated primary motor cortex lesion monkeys [27,28,33]. In particular, post-treatment the monkeys exhibited an improved recovery of original dexterity movements, i.e. the precision grip, especially for the challenging horizontal slots in the modified Brinkman board task [33]. This therapy induced behavioral improvement, reflected by refinement of motor control, may be in part related to the presently observed minimization of the loss of the cortico-basal ganglia and cortico-cerebellar loops in treated monkeys as compared to untreated monkeys (Fig. 3), although other mechanisms may be involved. Besides the enhancement of functional motor recovery due to anti-Nogo-A antibody treatment after primary motor cortex lesion [27,28,33], other treatments were reported to promote recovery in various models of motor cortex lesion in non-human primates [26,34,41,42,44,46,104-109].

Considering interindividual variability, differences in sizes and positions of tracers' injections, differences in thalamus nomenclatures, etc, the distributions of thalamocortical neurons projecting to the premotor cortex in the large sense across the various thalamic nuclei (Table 2) are largely consistent with previous studies, at least for intact monkeys [59,79,82,110-117]. In the primary motor cortex lesioned monkeys, the general distribution of BDA-labelled thalamocortical neurons across the thalamic nuclei was not dramatically modified, except a trend toward an increase of thalamocortical neurons in the ventrolateral nucleus (VL), to the detriment of other thalamic nuclei, such as the ventroanterior nucleus (VA), as compared to intact monkeys. The BDA injections in the premotor cortex were targeted to the dorsal and ventral divisions (PMd and PMv), except in 3 monkeys with BDA injections restricted to the dorsal division (PMd; see Table 1). More precisely, in each of the dorsal and ventral divisions of the premotor cortex, the BDA injections spread more on their caudal portions (PMd-c and PMv-c) than on their rostral counterparts (PMd-r and PMv-r). This bias towards the caudal parts of the premotor cortex is consistent with the percentages of thalamocortical neurons observed in the thalamic nucleus MD (ranging mostly around 10-15%; see Table 2), in line with a previous report for PMd-c and PMv-c [82], while the percentages in MD were clearly higher (20-40%) when the tracers injections were targeted to the rostral parts of PMd and PMv (PMd-r and PMv-r) [82].

Although the total number of monkeys (n=10) involved in the present study is reasonable considering the ethical restrictions to use non-human primates for biomedical research, an obvious limitation is of course the small number of animals in each of the 3 subgroups to be compared (n=3, n=4 and n=3, respectively; see Table 1 and Fig. 3). These small numbers of subjects after stratification in 3 subgroups prevent the application of meaningful statistical approaches to support the observation of visually perceived large segregation between the 3 subgroups (Fig. 3). The question remains whether larger subgroups of subjects would still result in the absence of overlap between the 3 subgroups after normalization of the labelled thalamocortical neurons' numbers (Fig. 3). Another limitation of the present study

is the lack of obvious scenario explaining the loss of thalamocortical neurons projecting to the intact ipsilesional premotor cortex after primary motor cortex lesion. One possibility, considering the partial overlap in the thalamus of the territories projecting to the primary and premotor cortices in intact animals [82], is that some thalamocortical neurons individually send axonal diverging projections simultaneously to the primary motor cortex and to the premotor cortex. A lesion of the primary motor cortex may generate a retrograde degeneration, eliminating the cell body of origin, which would result in a loss of the associated thalamocortical input to the premotor cortex as well (by loss of the axon collateral to the premotor cortex). This mechanism is however not quantitatively supported by the data presented in Figure 4. The more extensive the lesion of the primary motor cortex, the larger the loss of thalamocortical neurons by retrograde degeneration would be expected, based on such scenario. On the contrary, as illustrated in Figure 4, the loss of thalamocortical neurons projecting to the premotor cortex was largely independent from the primary motor cortex lesion size. Other mechanisms, mostly indirect may also come into play, although largely unknown. The minimizing effect on the decrease of thalamocortical projections by the anti-Nogo-A antibody treatment is most likely due to its action on connections' rewiring, via regenerative sprouting and/or compensatory sprouting [39,80,81]. The connectivity changes as a result of a brain lesion are most probably widespread and complex. A comparison between distinct studies must be done with great care, as small variability in the experimental parameters (e.g. size and precise position of the lesion, extent and location of tracers' injection sites, time interval between lesion and tracers' injection, ipsilesional versus contralesional hemisphere) may strongly affect the scenario of rewiring. For instance, after lesion restricted to the primary motor cortex, the corticobulbar projection from the homolesional intact premotor cortex was downregulated [74] while, after a large lesion including the primary motor cortex, the premotor cortex and part of the parietal cortex, the corticobulbar projection from the supplementary motor cortex (SMA) was upregulated as compared to controls and to monkeys with a lesion restricted to the primary and premotor cortices [118].

The present study emphasizes the notion that, following a lesion of the primary motor cortex, functional reorganization and rewiring of connectivity are not restricted to cortical level, but also take place subcortically, including the thalamus. Indeed, the anti-Nogo-A antibody treatment applied here had an effect opposing to some extent the massive loss of thalamocortical neurons projecting to the premotor cortex observed in untreated monkeys, following lesion of the primary motor cortex. In other words, the motor thalamus may also play a role in the functional recovery, especially when a treatment enhanced the functional recovery [33]. Besides the thalamus, other subcortical motor centers may be involved in the functional recovery of manual dexterity following motor cortex lesion, such as the reticular formation and the red nucleus [119-123].

Conclusions

Several tract-tracing studies in non-human primates have investigated the changes of connectivity of the intact premotor cortex after lesion of the adjacent primary motor cortex, as far as corticocortical connections and efferent projections are concerned (see above). For the first time, the present study reports on changes affecting the afferent thalamocortical projection to the premotor cortex after primary motor cortex lesion. The thalamocortical projection to the premotor cortex was strongly reduced, as compared to intact monkeys. This strong reduction was moderately attenuated by an anti-Nogo-A antibody treatment. As other connectional changes, the present effect of the primary motor cortex lesion on the long term on the thalamocortical projection to the premotor cortex may contribute to the behavioral adaptation in the form of an incomplete functional recovery of manual dexterity. Future work, using selective inactivation techniques, is needed to confirm the notion that the decrease of the thalamocortical projection to the premotor cortex may support part of the functional recovery. Moreover, more advanced tract-tracing methods based on viruses may have the potential to reveal and quantify at once all the connectivity changes following a specific brain or spinal cord lesion, by visualizing distinct axons trajectories and neuronal subpopulations in transparency of the brain, without sectioning the central nervous system [124-126], when this technology will become available for non-human primates. In particular, such global tract-tracing approaches will be highly valuable to quantify the connectivity changes affecting the massive corticofugal projections from the premotor cortex to the striatum (corticostriate projection) and to the thalamus (corticothalamic projection), following a lesion of the primary motor cortex.

Acknowledgments

The authors thank the precious contribution of former collaborators who contributed to the acquisition of the raw experimental data: Dr. S. Bashir, Dr. A. Belhaj-Saif, Dr. M. Kaeser, Dr. Y. Liu, Dr. A. Mir, Dr. J. Savidan, Prof. M. Schwab, Dr. A.F. Wyss. The authors wish to thank the technical assistance of Véronique Moret, Christine Roulin, Françoise Tinguely, Christiane Marti (histology and behavioral evaluations), Josef Corpataux, Laurent Bossy, Bernard Bapst and Bernard Morandi (animal house keeping), André Gaillard (mechanics), Bernard Aebischer (electronics), Laurent Monney (informatics).

Grant Sponsors: Swiss National Science Foundation, grants No 3130-025138, 31-28572.90, 31-43422.95, 31-61857.00, 310000-110005, 31003A-132465 (EMR), Novartis Foundation; The National Centre of Competence in Research (NCCR) on "Neural plasticity and repair".

Authors' contributions

AH and EMR designed the study and performed the experiments; AH analysed the histological sections; AH and EMR analysed the data and drafted the manuscript. The present study is derived from a previously unpublished chapter of Dr. Hamadjida's Ph.D. thesis at University of Fribourg (Switzerland).

Conflict of interest: The anti-Nogo-A antibody was provided by Novartis Pharma.

Data Availability: Original data are available on request to the corresponding author.

References

1. He S-Q, Dum RP, Strick PL. Topographic organization of corticospinal projections from the frontal lobe: Motor areas on the lateral surface of the hemisphere. *J Neurosci*. 1993; 13: 952-980.

2. He SQ, Dum RP, Strick PL. Topographic organization of corticospinal projections from the frontal lobe: motor areas on the medial surface of the hemisphere 71. *J Neurosci*. 1995; 15: 3284-3306.

3. Dum RP, Strick PL. Spinal cord terminations of the medial wall motor areas in macaque monkeys. *J Neurosci*. 1996; 16: 6513-6525.

4. Dum R, Strick P. Motor areas in the frontal lobe of the primate. *Physiol Behav*. 2002; 77: 677-682.

5. Luppino G, Rizzolatti G. The Organization of the Frontal Motor Cortex. *News in physiological sciences: an international journal of physiology produced jointly by the International Union of Physiological Sciences and the American Physiological Society* 2000;15: 219–224.

6. Rathelot JA, Strick PL Subdivisions of primary motor cortex based on cortico-motoneuronal cells. *Proc Natl Acad Sci USA* 2009; 106: 918-923.

7. Borra E, Belmalih A, Gerbella M, Rozzi S, Luppino G. Projections of the hand field of the macaque ventral premotor area F5 to the brainstem and spinal cord. *J Comp Neurol*. 2010; 518: 2570-2591.

8. Strick PL, Dum RP, Rathelot JA. The cortical motor areas and the emergence of motor skills: a neuroanatomical perspective. *Ann Rev Neurosci*. 2021; 44: 425-447.

9. Bufacchi RJ, Battaglia-Mayer A, Iannetti GD, Caminiti R. Cortico-spinal modularity in the parieto-frontal system: A new perspective on action control. *Prog Neurobiol*. 2023; 231:102537.

10. Lawrence DG, Kuypers HGJM. The functional organization of the motor system. I. The effects of bilateral pyramidal lesions. *Brain* 1968; 91: 1-14.

11. Lawrence DG, Hopkins DA. The development of motor control in the rhesus monkey: evidence concerning the role of corticomotoneuronal connections. *Brain* 1976; 99: 235–254.

12. Courtine G, Bunge MB, Fawcett JW, et al. Can experiments in nonhuman primates expedite the translation of treatments for spinal cord injury in humans? *Nat Med*. 2007; 13: 561-566.

13. Lemon RN. Descending pathways in motor control. *Ann Rev Neurosci*. 2008; 31: 195–218.

14. Lemon R. Recent advances in our understanding of the primate corticospinal system. *F1000 Research* 2019, 8 (F1000 Faculty Rev): 274 (https://doi.org/10.12688/f1000research.17445.1)

15. Griffin DM, Hoffman DS, Strick PL. Corticomotoneuronal cells are "functionally tuned". *Science* 2015; 350: 667-670.

16. Kinoshita M, Matsui R, Kato S, et al. Genetic dissection of the circuit for hand dexterity in primates. *Nature* 2012; 487: 235-238.

17. Yoshida Y, Isa T. Neural and genetic basis of dexterous hand movements. *Curr Opin Neurobiol*. 2018; 52: 25-32.

18. Nudo RJ, Milliken GW. Reorganization of movement representations in primary motor cortex following focal ischemic infarcts in adult squirrel monkeys. *J Neurophysiol*. 1996; 75, 2144-2149.

19. Nudo RJ, Wise BM, SiFuentes F, Milliken GW Neural Substrates for the Effects of Rehabilitative Training on Motor Recovery After Ischemic Infarct. *Science* 1996; 272: 1791-1794.

20. Liu Y, Rouiller EM. Mechanisms of recovery of dexterity following unilateral lesion of the sensorimotor cortex in adult monkeys. *Exp Brain Res*. 1999; 128, 149-159.

21. Murata Y, Higo N, Oishi T, Yamashita A, Matsuda K, Hayashi M, Yamane S. Effects of Motor Training on the Recovery of Manual Dexterity After Primary Motor Cortex Lesion in Macaque Monkeys. *J Neurophysiol*. 2008; 99:773-786.

22. Murata Y, Higo N, Hayashi T, et al. Temporal Plasticity Involved in Recovery **from** Manual Dexterity Deficit after Motor Cortex Lesion in Macaque Monkeys. *J Neurosci*. 2015; 35: 84-95.

23. Darling WG, Pizzimenti MA, Rotella DL, et al. Volumetric effects of motor cortex injury on recovery of dexterous movements. *Exp Neurol*. 2009; 220:90-108.

24. Darling WG, Helle N, Pizzimenti MA, et al. Laterality affects spontaneous recovery of contralateral hand motor function following motor cortex injury in rhesus monkeys. 2013. *Exp Brain Res*. 228:9-24.

25. Darling WG, Morecraft RJ, Rotella D, et al. Recovery of precision grasping after motor cortex lesion does not require forced use of the impaired hand in macaca mulatta. *Exp Brain Res*. 2014; 232: 3929-3938.

26. Kaeser M, Brunet JF, Wyss AF, et al. Autologous adult cortical cell implantation enhanced functional recovery of manual dexterity after unilateral lesion

of motor cortex in non-human primates. *Neurosurg.* 2011; 68: 1405-1417.

27. Wyss AF, Hamadjida A, Savidan J, et al. Long-term motor cortical map changes following unilateral lesion of the hand representation in the motor cortex in macaque monkeys showing functional recovery of hand functions. *Restor Neurol. Neurosci.* 2013; 31: 733-760.

28. Hoogewoud F, Hamadjida A, Wyss AF, et al. Comparison of functional recovery of manual dexterity after unilateral spinal cord lesion or motor cortex lesion in adult macaque monkeys. *Front Neurol.* 2013, 4: 101. doi: 10.3389/fneur.2013.00101

29. Bottenfield KR, Bowley BGE, Pessina MA, Medalla M, Rosene DL, Moore TL. Sex differences in recovery of motor function in a rhesus monkey model of cortical injury. *Biol Sex Differ.* 2021; 1254: 1-15.

30. LeFriec A, Desmoulin F, Demain B, et al. A reproducible new model of focal ischemic injury in marmoset monkey: MRI and behavioral follow-up. *Transl Stroke Res.* 2021; 12: 98-111.

31. Frost SB, Chen D., Barbay S, Friel KM, Plautz EJ, Nudo RJ. Reorganization of Ventral Premotor Cortex After Ischemic Brain Injury: Effects of Forced Use. *Neurorehab Neural Repair* 2022; 36: 514-524.

32. Plautz, E.J., Barbay S, Frost SB, et al. Spared Premotor Areas Undergo Rapid Nonlinear Changes in Functional Organization Following a Focal Ischemic Infarct in Primary Motor Cortex of Squirrel Monkeys. *J Neurosci.* 2023; 43: 2021-2032.

33. Rouiller EM. Re-examination and extension of manual dexterity behavioral data in M1 lesioned adult macaque monkeys: a survey of therapies induced enhancement of functional recovery. *Neurosci Insights* 2026; https://doi.org/10.1177/26331055261421348

34. Roux C, Savidan J, Brunet JF, et al. Confirmation of the enhancement effect of ANCE treatment on functional recovery of manual dexterity from primary motor cortex (M1) lesion in adult macaque monkeys. *Brain Behavior* 2025; 15:e70986: 1-14. https://doi.org/10.1002/brb3.70986

35. Frost SB, Barbay S, Friel KM, Plautz EJ, Nudo RJ. Reorganization of Remote Cortical Regions After Ischemic Brain Injury: A Potential Substrate for Stroke Recovery. *J Neurophysiol.* 2003; 89: 3205-3214.

36. Dancause N, Barbay S, Frost SB, et al. Extensive cortical rewiring after brain injury. *J Neurosci.* 2005; 25: 10167-10179.

37. Dancause, N., Barbay S, Frost SB, et al. Effects of small ischemic lesions in the primary motor cortex on neurophysiological organization in ventral premotor cortex. *J Neurophysiol.* 2006; 96: 3506-3511.

38. Dancause N, Nudo RJ. Shaping plasticity to enhance recovery after injury. *Progr Brain Res.* 2011; 192: 273-295.

39. Hamadjida A, Wyss AF, Mir A, Schwab ME, Belhaj-Saif A, Rouiller EM. Influence of anti-Nogo-A antibody treatment on the reorganization of callosal connectivity of the premotor cortical areas following unilateral lesion of primary motor cortex (M1) in adult macaque monkeys. *Exp Brain Res.* 2012; 223: 321-340.

40. Nudo RJ. Recovery after brain injury: mechanisms and principles. *Front Hum Neurosci.* 2013; 7: 887: 1-14.

41. Plautz EJ, Barbay S, Frost SB, et al. Effects of subdural monopolar cortical stimulation paired with rehabilitative training on behavioral and neurophysiological recovery after cortical ischemic stroke in adult squirrel monkeys. *Neurorehab Neural Repair* 2016; 30: 159-172.

42. Orczykowski ME, Arndt KR, Palitz LE, et al. Cell based therapy enhances activation of ventral premotor cortex to improve recovery following primary motor cortex injury. *Exp Neurol.* 2018; 305: 13-25.

43. Yamamoto T, Hayashi T, Murata Y, Ose T, Higo N. Premotor Cortical-Cerebellar Reorganization in a Macaque Model of Primary Motor Cortical Lesion and Recovery. *J Neurosci.* 2019; 39: 8484-8496.

44. Medalla M, Chang W, Calderazzo SM, et al. Treatment with Mesenchymal-Derived Extracellular Vesicles Reduces Injury-Related Pathology in Pyramidal Neurons of Monkey Perilesional Ventral Premotor Cortex. *J Neurosci.* 2020; 40: 3385-3407.

45. Moreau-Debord I, Serrano E, Quessy S, Dancause N. Rapid and Bihemispheric Reorganization of Neuronal Activity in Premotor Cortex after Brain Injury. *J Neurosci.* 2021; 41: 9112-9128.

46. Calderazzo S, Covert M, De Alba D, et al. Neural recovery after cortical injury: Effects of MSC derived extracellular vesicles on motor circuit remodeling in rhesus monkeys. *IBRO Neurosci Reports* 2022; 13: 243-254.

47. Borgognon S, Rouiller EM. Loss of motor cortical inputs to the red nucleus after CNS disorders in nonhuman primates. *J Neurosci.* 2023; 43: 1682-1891. doi: 10.1523/JNEUROSCI.1942-22.2023.

48. Rouiller EM. Adaptation of the layer V supraspinal motor corticofugal projections from the primary

(M1) and premotor (PM) cortices after CNS motor disorders in non-human primates: A survey. *Transl Neurosci.* 2024; 15: 20220342. https://doi.org/10.1515/tnsci-2022-0342.

49. Alexander GE, DeLong MR, Strick PL. Parallel Organization of Functionally Segregated Circuits Linking Basal Ganglia and Cortex. *Ann Review Neurosci.* 1986; 9: 357–381. https://doi.org/10.1146/annurev.ne.09.030186.002041.

50. Hoover JE. Strick PL. Multiple output channels in the basal ganglia. *Science* 1993; 259: 819 -821.

51. Hoover JE, Strick PL. The Organization of Cerebellar and Basal Ganglia Outputs to Primary Motor Cortex as Revealed by Retrograde Transneuronal Transport of Herpes Simplex Virus Type 1. *J Neurosci.* 1999; 19: 1446-1463.

52. Takada M, Tokuno H, Nambu A, Inase M. Corticostriatal Projections From the Somatic Motor Areas of the Frontal Cortex in the Macaque Monkey: Segregation Versus Overlap of Input Zones From the Primary Motor Cortex, the Supplementary Motor Area, and the Premotor Cortex. *Exp Brain Res.* 1998; 120: 114–128. https://doi.org/ 10.1007/s002210050384.

53. Middleton FA, Strick PL (2000) Basal ganglia and cerebellar loops: motor and cognitive circuits. *Brain Res Brain Res Rev.* 2000; 31: 236-250.

54. Dum RP, Strick PL. Transneuronal tracing with neurotropic viruses reveals network Microarchitecture. *Curr Opin Neurobiol.* 2013; 23: 245-249.

55. Gerbella M, Borra E, Mangiaracina C, Rozzi S, Luppino G. Corticostriate Projections from Areas of the "Lateral Grasping Network": Evidence for Multiple Hand-Related Input Channels. *Cereb Cortex* 2016; 26: 3096-3115.

56. Bostan AC, Strick PL. The basal ganglia and the cerebellum: nodes in an integrated network. *Nat Rev Neurosci.* 2018; 19: 338-350.

57. Gao Z, Davis C, Alyse M. Thomas AM, et al. A cortico-cerebellar loop for motor planning. *Nature* 2018; 563: 113-116.

58. Ueno S, Yamaguchi R, Isa K, et al. Supraspinal Plasticity of Axonal Projections From the Motor Cortex After Spinal Cord Injury in Macaques. *J Comp Neurol.* 2024; 532, e70007: 1-12.

59. Schell GR, Strick PL. The origin of thalamic inputs to the arcuate premotor and supplementary motor areas. *J Neurosci.* 1984; 4: 539-560.

60. Strick PL. How do the basal ganglia and cerebellum gain access to the cortical motor areas? *Behav Brain Res.* 1985; 18: 707-123.

61. Nambu A., Yoshida S, Jinnai K. Projection on the motor cortex of thalamic neurons with pallidal input in the monkey. *Exp Brain Res.* 1988; 71: 658-662.

62. Nambu A, Yoshida S, Jinnai K. (1991) Movement-related activity of thalamic neurons with input from the globus pallidus and projection to the motor cortex in the monkey. *Exp Brain Res.* 1991; 84: 279-284.

63. Orioli PJ, Strick PL. (1989) Cerebellr connections with the motor cortex and the arcuate premotor area: An analysis employing retrograde transneuronal transport of WGA-HRP. *J Comp Neurol.* 1989; 288: 612-626.

64. Tokuno H, Kimura M, Tanji J. Pallidal inputs to thalamocortical neurons projecting to the supplementary motor area: An anterograde and retrograde double labeling study in the macaque monkey. *Exp Brain Res.* 1992; 90: 635-638.

65. Ilinsky IA, Tourtellotte WG, Kultas-Ilinsky K. Anatomical distinction between the two basal ganglia afferent territories in the primate motor thalamus. *Stereotact Funct Neurosurg.* 1993; 60: 62-69.

66. Jinnai K, Nambu A, Tanibuchi I, Yoshida S. Cerebello- and pallido-thalamic pathways to areas 6 and 4 in the monkey. *Stereotact Funct Neurosurg.* 1993; 60: 70-79.

67. Rouiller EM, Liang F, Babalian A, Moret V, Wiesendanger M. Cerebello-thalamo-cortical and pallido-thalamo-cortical projections to the primary (M1) and supplementary (SMA) motor cortical areas: a multiple tracing study in macaque monkeys. *J Comp Neurol.* 1994; 345: 185-213.

68. Sakai ST, Inase M, Tanji J. The relationship between MI and SMA afferents and cerebellar and pallidal efferents in the macaque monkey. *Somatosens Mot Res.* 2002; 19: 139-148.

69. Sakai ST, Inase M, Tanji J. Comparison of cerebellothalamic and pallidothalamic projections in the monkey (Macaca fuscata): a double anterograde labeling study. *J Comp Neurol.* 1996; 368: 215-228.

70. Calzavara R, Zappalà A, Rozzi S, Matelli M, Luppino G. Neurochemical characterization of the cerebellar-recipient motor thalamic territory in the macaque monkey. *Eur J Neurosci.* 2005; 21: 1868-1894.

71. Evrard HC, Craig AD. Retrograde analysis of the cerebellar projections to the posteroventral part of

the ventral lateral thalamic nucleus in the macaque monkey. *J Comp Neurol*. 2008; 508: 286-314.

72. Fregosi M, Contestabile A, Hamadjida A, Rouiller EM. Corticobulbar projections from distinct motor cortical areas to the reticular formation in macaque monkeys. *Eur J Neurosci*. 2017; 45: 1379-1395.

73. Fregosi M, Rouiller EM. Ipsilateral corticotectal projections from the primary, premotor and supplementary motor cortical areas in adult macaque monkeys: a quantitative anterograde tracing study. *Eur J Neurosci*. 2017; 46: 2406-2415.

74. Fregosi M, Contestabile A, Badoud S, et al. Changes of motor corticobulbar projections following different lesion types affecting the central nervous system in adult macaque monkeys. *Eur J. Neurosci*. 2018; 48: 2050-2070.

75. Fregosi M, Contestabile A, Badoud S, et al. Corticotectal projections from the premotor or primary motor cortex after cortical lesion or Parkinsonian symptoms in adult macaque monkeys: a pilot study. *Front Neuroanat*. 2019; 13, Article 50: 1-11. Doi: 10.3389/fnana.2019.00050, p. 1-11.

76. Borgognon S, Cottet J, Badoud S, Bloch J, Brunet JF, Rouiller EM. Cortical Projection from the Premotor or Primary Motor Cortex to the Subthalamic Nucleus in Intact and Parkinsonian Adult Macaque Monkeys: A Pilot Tracing Study. *Front Neural Circuits* 2020; 14: 1-10. doi.org/10.3389/fncir.2020.528993

77. Gindrat AD, Wyss AF, Leuthard C, Rouiller EM, Kaeser M. Behavioral and connectional neuroplasticity in M1 lesion adult macaque monkeys. *Med Res Archives* 2025; 13: issue 10: 1-24. doi.org/10.18103/mra.v13i10.0000

78. Rouiller EM, A. Babalian A, O. Kazennikov O, V. Moret V, X.H. Yu XH, Wiesendanger M. Transcallosal connections of the distal forelimb representations of the primary and supplementary motor cortical areas in macaque monkeys. *Exp Brain Res*. 1994; 102: 227-243.

79. Rouiller EM, Tanné J, Moret V, Boussaoud D. Origin of thalamic inputs to the primary, premotor and supplementary motor cortical areas and to area 46 in macaque monkeys: a multiple retrograde tracing study. *J Comp Neurol*. 1999; 409: 131-152.

80. Schmidlin E, Wannier T, Bloch J, Rouiller E.M. Progressive plastic changes in the hand representation of the primary motor cortex parallels incomplete recovery from a unilateral section of the corticospinal tract at cervical level in monkeys. *Brain Res*. 2004; 1017: 172-183.

81. Schmidlin E, Wannier T, Bloch J, Belhaj-Saif A, Wyss A, Rouiller EM. Reduction of the hand representation in the ipsilateral primary motor cortex following unilateral section of the corticospinal tract at cervical level in monkeys. *BMC Neurosci*. 2005, 6: 56.

82. Morel A, Liu J, Wannier T, Jeanmonod D, Rouiller EM. (2005) Divergence and convergence of thalamocortical projections to premotor and supplementary motor cortex: a multiple tracing study in macaque monkey. *Eur J Neurosci*. 2005; 21: 1007-1029.

83. Wannier T, Schmidlin E, Bloch J, Rouiller EM. A unilateral section of the corticospinal tract at cervical level in primate does not lead to measurable cell loss in motor cortex. *J Neurotrauma* 2005; 22: 703-717.

84. Freund P, Schmidlin E, Wannier T, et al. Anti-Nogo-A treatment enhances corticospinal tract sprouting and functional recovery after unilateral cervical lesion in adult primates. *Nat Med*. 2006; 12: 790-792.

85. Freund P, Wannier T, Schmidlin E, et al. Anti-Nogo-A antibody treatment enhances sprouting of corticospinal (CS) axons rostral to an unilateral cervical cord lesion in adult macaque monkeys. *J Comp Neurol*. 2007; 502: 644-659.

86. Freund P, Schmidlin E, Wannier T, et al. Anti-Nogo-A antibody treatment promotes recovery of manual dexterity after unilateral cervical lesion in adult primates: re-examination and extension of behavioral data. *Eur J Neurosci*. 2009; 29: 983-996.

87. Kaeser M, Wyss AF, Bashir S, et al. Effects of unilateral motor cortex lesion on ipsilesional hand's reach and grasp performances in monkeys: relationship with recovery in the contralesional hand. *J Neurophysiol*. 2010; 103: 1630-1645.

88. Schwab ME. Nogo and axon regeneration. *Curr Opin Neurobiol*. 2004: 14,118–124.

89. Schwab ME. Functions of Nogo proteins and their receptors in the nervous system. *Nat Rev Neurosci*. 2010; 11: 799-811.

90. Liu J, Morel A, Wannier T, Rouiller EM Origins of callosal projection to the supplementary motor area (SMA): a direct comparison between pre-SMA and SMA-proper in macaque monkeys. *J Comp Neurol*. 2002; 443: 71-85.

91. Beaud ML, Schmidlin E, Wannier T, et al. Anti-Nogo-A antibody treatment does not prevent cell body shrinkage in the motor cortex in adult monkeys subjected to unilateral cervical cord lesion. *BMC Neurosci*. 2008; 9: 5.

92. 92 Contestabile A, Colangiulo R, Lucchini M, et al. Asymmetric and distant effects of a unilateral lesion

of the primary motor cortex on the bilateral supplementary motor areas in adult macaque monkeys. *J Neurosci*. 2018; 38: 10644-10656

93. Savidan J, Kaeser M, Belhaij-Saif A, Schmidlin E, Rouiller EM. Role of primary motor cortex in the control of manual dexterity assessed via a sequential bilateral lesion in the adult macaque monkey: a case study. *Neurosci*. 2017; 357: 303-324.

94. Molinari M, Hendry SH, Jones EG. Distributions of certain neuropeptides in the primate thalamus. *Brain Res*. 1987; 426: 270-289.

95. Rausell E, Jones E G. (1991) Chemically distinct compartments of the thalamic VPM nucleus in monkeys relay principal and spinal trigeminal pathways to different layers of the somatosensory cortex. *J Neurosci*. 1991; 11: 226-237.

96. Jones EG. Viewpoint: The core and matrix of thalamic organization. *Neurosci*. 1998; 85, 331-345.

97. Jones EG. The thalamic matrix and thalamocortical synchrony. *Trends Neurosci*. 2001; 24, 595-601.

98. Jones EG, Rubenstein JL. Expression of regulatory genes during differentiation of thalamic nuclei in mouse and monkey. *J Comp Neurol*. 2004; *477*, 55-80.

99. Jones EG. Neuroanatomy: Cajal and after Cajal. *Brain Res Rev*. 2007; *55*, 248-255.

100. Gerfen CR, Bolam P The neuroanatomical organization of the basal ganglia. In: Handbook of basal ganglia structure and function (Steiner H, Tseng KY, eds) 2010, pp 3–32. Amsterdam: Elsevier.

101. Borra E, Rizzo M, Gerbella M, Rozzi S, Luppino G. Laminar Origin of Corticostriatal Projections to the Motor Putamen in the Macaque Brain. *J Neurosci*. 2021; 41: 1455-1469.

102. McNeal DW, Darling WG, Ge J, et al. Selective Long-Term Reorganization of the Corticospinal Projection From the Supplementary Motor Cortex Following Recovery From Lateral Motor Cortex Injury. *J Comp Neurol*. 2010; 518: 586-621.

103. Morecraft RJ, Ge J, Stilwell-Morecraft KS, et al. Frontal and Frontoparietal Injury Differentially affect the Ipsilateral Corticospinal Projection from the Non-lesioned Hemisphere in Monkey (*Macaca mulatta*). *J Comp Neurol*. 2016; 524: 380-407.

104. Moore TL, Pessina MA, Finklestein SP, Kramer BC, Killiany RJ, Rosene DL. Recovery of Fine Motor Performance After Ischemic Damage to Motor Cortex Is Facilitated by Cell Therapy in the Rhesus Monkey. *Somatos Motor Res*. 2013; 30: 185–196. https://doi.org/10.3109/08990220.2013.790806.

105. Moore TL, Pessina MA, Finklestein SP, et al. 2016. Inosine Enhances Recovery of Grasp Following Cortical Injury to the Primary Motor Cortex of the Rhesus Monkey. *Restor Neurol Neurosci*. 2016; 34: 827–848. https://doi.org/10.3233/RNN-160661.

106. Moore TL, Bowley BGE, Pessina MA, et al. 2019. Mesenchymal Derived Exosomes Enhance Recovery of Motor Function in a Monkey Model of Cortical Injury. *Restor Neurol Neurosci*. 2019; 37: 347–362. https://doi.org/10.3233/RNN-190910.

107. Barbay S, Plautz EJ, Elena Zoubina E, Frost SB, Cramer SC, Nudo RJ. Effects of Postinfarct Myelin-Associated Glycoprotein Antibody Treatment on Motor Recovery and Motor Map Plasticity in Squirrel Monkeys. *Stroke* 2015; 46: 1620-1625.

108. Kim EH, Son JP, Oh GS, et al. Clinical Scale MSC-Derived Extracellular Vesicles Enhance Poststroke Neuroplasticity in Rodents and Non-Human Primates. *J Extracell Vesicles* 2025; 14: e70110. https://doi.org/10.1002/jev2.70110.

109. McCann RP, Bowley B, Pessina MA, et al. Reduction of Inflammatory Biomarkers Underlies Extracellular Vesicle Mediated Functional Recovery in an Aged Monkey Model of Cortical Injury. *Front. Aging Neurosci.* 2025; 17: 1605144. https://doi.org/10.3389/fnagi.2025.1605144.

110. Goldman-Rakic PS, Porrino LJ. The primate mediodorsal (MD) nucleus and its projection to the frontal lobe. *J Comp Neurol*. 1985; 242: 535-560.

111. Jones EG. Ascending inputs to, and internal organization of, cortical motor areas. In CIBA Foundation (ed), *Motor areas of the cerebral cortex*. John Wiley & Sons, New-York, 1987; pp. 21-39.

112. Matelli M, Luppino G, Fogassi L, Rizzolatti G. Thalamic input to inferior area 6 and area 4 in the macaque monkey. *J Comp Neurol*. 1989; 280: 468-488.

113. Darian-Smith C, Darian-Smith I, Cheema SS. Thalamic projections to sensorimotor cortex in the macaque monkey: use of multiple retrograde fluorescent tracers. *J Comp Neurol*. 1990; 299: 17-46.

114. Nakano K, Tokushige A, Kohno M, Hasegawa Y, Kayahara T, Sasaki K. An autoradiographic study of cortical projections from **motor** thalamic nuclei in the macaque monkey. *Neurosci Res*. 1992; 13: 119-137.

115. Kurata K. Site of origin of projections from the thalamus to dorsal versus ventral aspects of the premotor cortex of monkeys. *Neurosci Res*. 1994; 21: 71–76.

116. Matelli M, Luppino G. Thalamic input to mesial and superior area 6 in the macaque monkey. *J Comp Neurol*. 1996; 372: 59-86.

117. McFarland NR, Haber SN. Thalamic Relay Nuclei of the Basal Ganglia Form Both Reciprocal and Nonreciprocal Cortical Connections, Linking Multiple Frontal Cortical Areas. *J Neurosci*. 2002; 22: 8117-8132.

118. Darling WG, Ge J, Morecraft KSS, Rotella DL, Pizzimenti MA, Morecraft RJ. Hand motor recovery following extensive frontoparietal cortical injury is accompanied by upregulated corticoreticular projections in monkey. *J Neurosci*. 2018; 38: 6323–39.

119. Fetz EE, Cheney PD, Mewes K, Palmer S. Control of forelimb muscle activity by populations of corticomotoneuronal and rubromotoneuronal cells. *Prog Brain Res*. 1989: 80: 437-449, discussion 427-430.

120. Zaaimi B, Soteropoulos DS, Fisher KM, Riddle CN, Baker SN. Classification of neurons in the primate reticular formation and changes after recovery from pyramidal tract lesion. *J Neurosci*. 2018; 38: 6190–206.

121. Zaaimi B, Dean LR, Baker SN. Different contributions of primary motor cortex, reticular formation, and spinal cord to fractionated muscle activation. *J Neurophysiol*. 2018; 119: 235-250.

122. Glover IS, Baker SN. Cortical, corticospinal, and reticulospinal contributions to strength training. *J Neurosci*. 2020; 40: 5820-5832.

123. Glover IS, Baker SN. Both corticospinal and reticulospinal tracts control force of contraction. *J Neurosci*. 2022; 42: 3150-3164.

124. Attarpour A, Osmann J, Rinaldi A, et al. A deep learning pipeline for three-dimensional brain-wide mapping of local neuronal ensembles in teravoxel light-sheet microscopy. *Nat Meth*. 2025; 22: 600-611. https://doi.org/10.1038/s41592-024-02583-1

125. Chapman PD, Kulkarni AS, Trevisan AJ, et al. A brain-wide map of descending inputs onto spinal V1 interneurons. *Neuron* 2025; 113: 524-538.

126. Attarpour A, Raffiee M, Xu T, et al. Quantitative profiling of whole-brain connectomes at single-axon resolution using deep learning and high-resolution light sheet microscopy. bioRxiv [Preprint]. 2025 Nov 16:2025.11.14.688340. doi:10.1101/2025.11.14.688340.